Image Enhancement And Denoising Under Max/Min Flow Framework

Hongchuan Yu, Chin-Seng Chua
School of Electrical and Electronic Engineering,
Nanyang Technological University, Singapore, Email:ehcyu@ntu.edu.sg

Abstract: In this paper, the Max/Min flow scheme for image enhancement and denoising is firstly studied, and the speckle problem is solved under our proposed reformulated Max/Min flow scheme. Furthermore, it is proved that the continued application of the original scheme erodes all structures or boundaries for the grey-level (or color) image. In order to control smoothing effect, the zero-crossing detector and GVF field are introduced in the curvature flow respectively, so that the proposed schemes can reach a steady state solution, and the final steady state images maintain the essential structures of the shape while the small oscillations are smoothed out.

1. INTRODUCTION

Since the eighties, linear and nonlinear PDE's models have been introduced into image restoration and analysis as multi-resolution techniques. Of interest are the studies on the image anisotropic diffusion, in which the smoothing has to be adaptively controlled by the amount of smoothing and the direction along the image features respectively, such as Perona-Malik equation [1], shock filter [2], etc. The directional control is concerned at all times. Based on the total variation (TV) norm, the diffusion equation is written as a divergence form [3], $I_t = \frac{I_{\xi\xi}}{|\nabla I|} = \nabla \cdot \frac{\nabla I}{|\nabla I|}$, where $I_{\xi\xi}$ is the second derivative of intensity in the direction orthogonal to the gradient. For noise elimination, the diffusion equation in [4] is defined as, $I_t = \frac{I_{\xi\xi}}{|\nabla G_\sigma * I|}$, where the first difference operator of Gaussian ∇G_σ enhances the boundaries of the shape. It has been proved that this diffusion equation is well-posed in the space of bounded variation. The similar model is also proposed in [8] independently. If an image is interpreted as a collection of iso-intensity contours which can be evolved, it is obvious that the divergence form of $I_{\xi\xi}$ can be interpreted as the curvature of intensity contour [6,7], $\kappa = \nabla \cdot \frac{\nabla I}{|\nabla I|}$. This leads to a kind of diffusion equations, which is called the geometric curvature flow in the front propagation, and written as $I_t = \kappa |\nabla I|$. In [5], Chen et al. generalized the curvature motion as image multi-scale analysis model, $I_t = F(\kappa)|\nabla I|$, where F is an increasing function of its curvature, and presented the proof of the uniqueness and existence of its viscosity solution. Usually, the speed function F is defined as one of the following two forms $F(\kappa) = \kappa$ or $F(\kappa) = \sqrt[3]{\kappa}$. The former is called the curvature flow, the later is called affine invariant flow [9], which permits to get the affine invariance. In order to enhance the image and remove noise without too much blurring, the Max/Min flow scheme is first proposed in [6]. Unfortunately, the implementation of this scheme contains a numerical problem that some speckle will appear in the grey-level (or color) image and contaminate the entire image gradually. An example is shown in Fig.2(a-c).

In addition, we wish a steady state image could be obtained, which removes noise while preserving the interesting boundaries simultaneously. In other words, we hope that the Max/Min flow scheme can reach a steady state solution. Unfortunately, it is not always guaranteed. In this paper, we proved that all the structures would be smoothed out under the original Max/Min flow scheme. In our presented schemes, the second derivate zero-crossing detector and the gradient vector flow (GVF) field [10] are introduced in the curvature flow under the Max/Min flow framework respectively, so that these modified schemes can reach trivial steady state solutions. However, the Max/Min flow framework is a flexible computational framework, and many methods and strategies can be combined into this framework.

This paper is organized as follows: in section 2, the Max/Min flow scheme is briefly introduced. In section 3, the Max/Min flow scheme is reformulated to overcome the above speckle problem. In section 4, it is proved that the continued application of the original scheme would erode all structures or boundaries for the grey-level (or

color) image. In order to obtain a steady state solution, the GVF field and the second derivate zero-crossing detector are introduced in the curvature flow under the Max/Min flow framework respectively in section 5. Finally, our conclusions appear in section 6.

2. MAX/MIN FLOW SCHEME

The Max/Min flow scheme was first introduced in [6] for the grey scale, texture and color image enhancement and noise removal. An image is interpreted as a collection of iso-intensity contours which can be evolved. The level set equation of image intensity *I* can be written as,

$$I_t = F|\nabla I| \tag{1}$$

where,

$$F = \begin{cases} \max(\kappa,0), & \text{average}(I(X), X \in \Omega) < Threshold \\ \min(\kappa,0), & otherwise \end{cases},$$

where Ω is a neighborhood around some point. The above definition of speed function is called the Max/Min flow framework. For the binary images, the threshold is simply taken as the average of the two intensity values. Whereas, for the grey-scale and texture images, the threshold should be estimated as the average value of the intensity obtained along the direction perpendicular to the gradient direction in the neighborhood Ω. Let the interior intensity of the shape be less than the exterior ones. The particular behavior of the max flow and min flow are respectively described in the following properties, (see [6,7] for detail)

Property 1: The flow under $F = \min(\ ,0)$ allows the inward concave fingers to grow outward, while suppressing the motion of the outward convex regions. And the motion halts as soon as the convex hull is obtained.

Property 2: The flow under $F = \max(\ ,0)$ allows the outward convex regions to grow inward while suppressing the motion of the inward concave regions. Once the shape becomes fully convex, the flow becomes the same as regular curvature flow, in which case the shape collapses to a point.

In fact, the key idea of the Max/Min flow scheme is to select the correct choice of flow that both smoothes out small oscillations, while maintains the essential details of the shape.

3. ANALYSES AND SOLUTION OF SPECKLE PROBLEM

The speckle problem appearing in implementation of the scheme (1) results from the texture or noise in images. It is a numerical drawback.

First, we imagine the binary case where there are only two grey levels in an image: one is object intensity, and another is background intensity. Suppose that the background color is lighter than the object color, i.e. its intensity value is greater than the object one. The threshold in Eq.(1) is defined as the average of these two intensity values (see Fig. 1). Let some intensity contour pass the point A, and the circle range is the neighborhood around point A. If point A belongs to the object region, the smoothing takes place. Since the threshold is greater than the intensity average of $I(X)$ in the neighborhood around the point A, the max flow is chosen. And since the contour shape is convex, the curvature of point A is always positive, and the intensity contour moves inward the object region until the average becomes greater, and the "min" switch takes over. If point A belongs to the background region, no diffusion takes place. Since the threshold is less than the average, the min flow is chosen. But then the curvature of point A is positive, the speed is set to zero. Thus, no change occurs at the point A.

When the observed image is a gray scale or texture image, the analysis will become more complicated than the binary case. The threshold in Eq.(1) is defined as the average value of the intensity obtained in the tangential line, which is tangent to the intensity contour at point A (see Fig.1). Suppose that the threshold is greater than the average of the neighborhood and the curvature of point A is positive. Obviously, the intensity of point A should be updated. Because of the spurious edge, noise or numerical errors, it is possible that the intensity value of point A is greater than the threshold. Thus, its intensity value is updated as a greater one. After several iterations, the distinct highlight speckles will appear at point A. For the dark speckles, there is a similar analysis too.

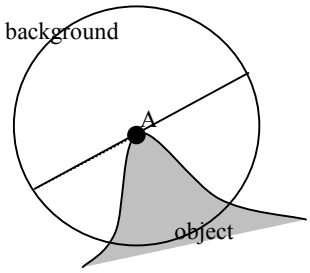

Fig. 1. The decision of max/min flow

In Fig.2(a-c), we illustrate the evolution results at different iteration steps. With continued application of scheme Eq.(1), the speckles will contaminate the whole images gradually. In order to overcome the above problem, the decision rule in Eq.(1) should be revised. According to the two properties in section 2, we know that the flow under $F = \max(\kappa,0)$ diffuses away all of the information while the flow under $F = \min(\kappa,0)$ preserves some of the structure. It is clear that when the average is less than the threshold, selecting the max flow

is to smooth out small oscillations, but not to enhance. Thus, any enhancement operation should be suppressed. According to the above analysis, we notice that the decision rule is too simple to select the correct choice between the max and min flows. So, the max/min flow can be re-defined as,

$$F=\begin{cases}\max(\kappa,0), & \begin{cases}\text{average}\big(X\in\Omega(Y)\big)<Threshold\\ I(Y)<Threshold\end{cases}\\ 0, & otherwise\\ \min(\kappa,0), & \begin{cases}\text{average}\big(X\in\Omega(Y)\big)>Threshold\\ I(Y)>Threshold\end{cases}\end{cases} \quad (2)$$

Obviously, when the threshold is greater than the average, but the intensity of point A is greater than the threshold, the speed function is set to zero. So, no speckle appears at point A. The experiment result is shown in Fig.2(d).

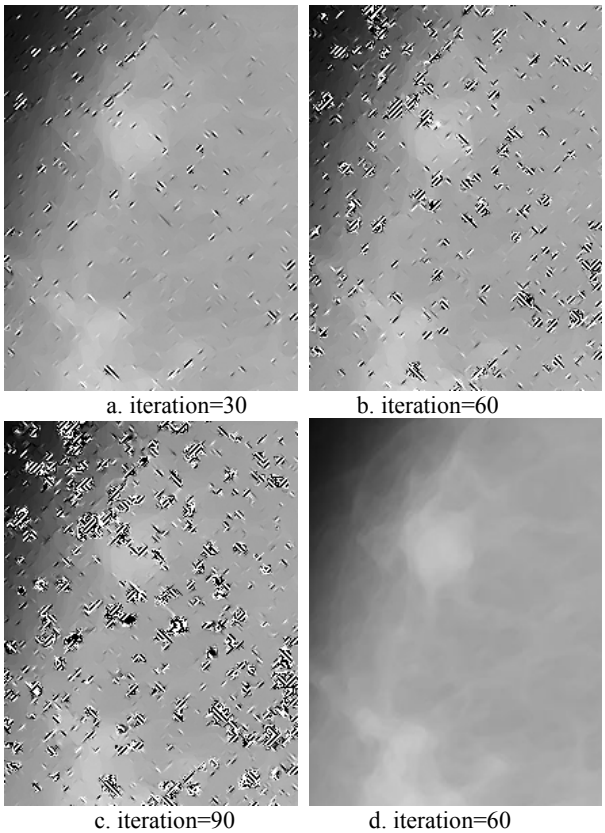

a. iteration=30 b. iteration=60

c. iteration=90 d. iteration=60

Fig. 2. The speckles appear using Eq.(1) in (a-c), but they could be suppressed by Eq.(2) in (d).

4. CURVATURE EQUATION UNDER MAX/MIN FLOW FRAMEWORK

As a kind of anisotropic diffusion model, the curvature flow contains a few particular geometric and numerical advantages. The most attractive quality of this kind of approaches is that sharp boundaries are preserved. According to Grayson's theorem, we know that all information is eventually removed through continued application of the curvature flow scheme. In order to preserve some important features after continued application of the curvature flow scheme, the Max/Min scheme is introduced in the speed function [6,7]. We will prove that this expectation could not be guaranteed under the scheme of Eq.(1).

First, consider the definition of the speed function. We wish the scheme of Eq.(1) could reach a steady state solution, i.e. $I_t = 0$. Roughly speaking, we might think that the final solution (intensity $I(X)$) be a harmonic function, and that the curvature flow could lead Eq.(1) towards a harmonic solution. According to the mean value theorem for harmonic functions, we know that the isolated noise points and notch shaped structure in the neighborhood around some point would be smoothed out gradually. It is easy to verify that the inflectional shape or boundary in the neighborhood will gradually become straight or die out according to the definition of the speed function in Eq.(1). They are illustrated in Fig.3. Thus, we have,

Proposition 1: The speed function in Eq.(1) will result in the edges or boundaries of shape tending to straight.

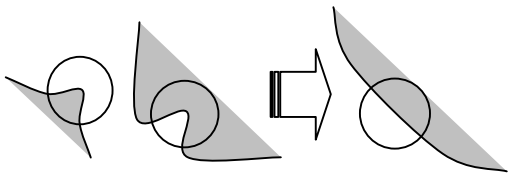

Fig.3 The boundary of shape tending to straight, where the circle is a neighborhood around some point

Then, we consider the continued application of the scheme of Eq.(1). It is expected that all oscillations below some radius level be removed, while all features above that level are preserved; and the algorithm can stop automatically once the sub-scale noise is removed. Unfortunately, it isn't able to accomplished in practice.

Suppose that after enough iteration steps, all oscillations below some radius (it is also the radius of neighborhood around some point) are removed. In other word, the inflection edge becomes straight line in the neighborhood around every point that is on the boundaries of shapes according to the proposition 1, while all the features above that radius will be preserved. This supposition is described as follows.

Assume that L is a bending boundary above some radius r, and the circle is the neighborhood around some point $\forall \mathbf{x}\in L$ (see Fig.4). Point $\mathbf{x}_1$ is far away from point $\mathbf{x}_n$. In the neighborhood around points $\mathbf{x}_1, \mathbf{x}_n$, the two

segments of L are both straight lines, $\overline{A_1B_1}, \overline{A_nB_n} \subset L$, whose extension lines intersect at point C.

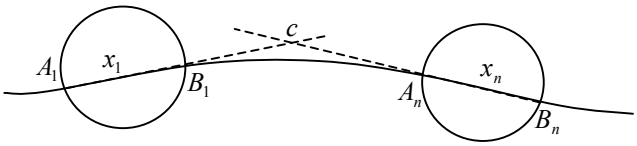

Fig.4 The edge L in a steady state image

Let the increment $|\Delta\mathbf{x}| \le r$ is small enough, so that the new segment of L, $\overline{A_2B_2}$, in the neighborhood around point $\mathbf{x}_2 = \mathbf{x}_1 + \Delta\mathbf{x} \in L$ is a straight line. Then, $A_2 = A_1 + \Delta\mathbf{x}, B_2 = B_1 + \Delta\mathbf{x}$, and $A_2, B_2 \in L$. Obviously, after the limited extension steps m, $\begin{cases} \mathbf{x}_m = \mathbf{x}_{m-1} + \Delta\mathbf{x} \\ A_m = A_{m-1} + \Delta\mathbf{x}, \ \mathbf{x}_m, \mathbf{x}_{m-1}, A_m, A_{m-1}, B_m, B_{m-1} \in L \\ B_m = B_{m-1} + \Delta\mathbf{x} \end{cases}$, we have $B_m = C$. Similar extension procedure is applied to point $\mathbf{x}_n$. After the limited extension steps p, we have $A_p = C$, i.e. $B_m = A_p$, and $A_m, \mathbf{x}_m, B_p, \mathbf{x}_p, C \in L$. Then, in the neighborhood around point C, the two segments of L, $\overline{\mathbf{x}_mC}$ and $\overline{\mathbf{x}_pC}$, should have the same slope. In other words, the two line segments $\overline{A_1B_1}$ and $\overline{A_nB_n}$ also have the same slope. Thus, the straight lines $\overline{A_1C}$ and $\overline{B_nC}$ overlap, and $\overline{A_1C}, \overline{B_nC} \subset L$. It is clear that the edge L must be straight line. This conclusion conflicts with the initial supposition. Hence, L must be a straight line.

If the length of L is limited, there is a corner at the ends of L. Continued application of scheme Eq.(1) smoothes out these corners, and results in diffusing away all of the structures. From the above analysis, we conclude the following proposition,

Proposition 2: The final steady state solution of scheme Eq.(1) should be the following two cases:

1) If the inflection edge becomes straight line in the neighborhood with arbitrary radius level around every point that is on the boundaries of shapes, the edge of shape must be a straight line over the boundary of the whole image;
2) otherwise, all the features are smoothed out.

The regular curvature equation usually satisfies the maximum/minimum principle, i.e. the solution does not have local maximum or minimum at time $t > 0$, and the global extrema are bounded by these of the initial and boundary conditions. The boundary conditions usually refer to Neumann boundary conditions ($\frac{\partial I}{\partial \mathbf{n}} = 0$ where $\mathbf{n}$ is the direction of gradient). Obviously, the global extreme occurs at initial time, i.e. $I_0(\mathbf{x})$. And the steady state solution should be a constant function. The Grayson theorem implies that the shapes or boundaries driven by the curvature flow will collapse to a point, and all information die out. This is the steady state solution of the regular curvature equation. It is clear that the decision rule in Eq.(1) results in the same steady state solution as one of the regular curvature flow.

Another interested phenomenon is that many continued iteration of scheme Eq.(1) with some small radius is roughly similar to one application of scheme Eq.(1) with some large radius. Assume that the length of some edge l is greater than a radius, $|l| > r$, no diffusion takes place at the center of l, while the smoothing takes place at the two ends of l under the scheme of Eq.(1). It can be noticed that the length of l is becoming less and less with continued application of scheme Eq.(1). When $|l| < r$, the diffusion takes place at center of l. The edge l is smoothed out. If the radius is selected so large that the initial edge l satisfies $|l| < r$ at the beginning, it is obvious that diffusion takes place at every point on l. The edge l will be smoothed out quickly. So, we have,

Proposition 3: Iteration of scheme Eq.(1) with a small radius is roughly the same as one evolution with a large radius.

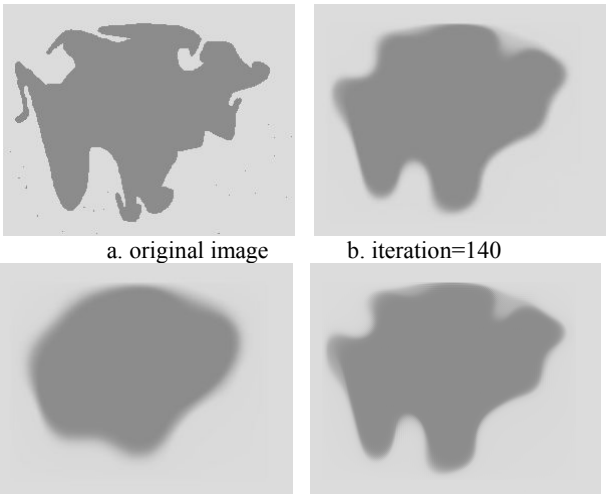

a. original image b. iteration=140

c. iteration=360 d. iteration=80

Fig. 5. The comparison of evolution results between radius=1 and radius=5

In Fig.5(a-c), we illustrate the evolution of a simple grey image using Eq.(2) with radius=1. From Fig.5(a-c), it can be seen that the continued iteration of this Max/Min flow

will result in the erosion of the structure of the object. In addition, the evolution result for Eq.(2) with radius=5 is shown in Fig.5(d). It can be noticed that Fig.5(d) is similar to Fig.5(b) even with different numbers of iteration and radii.

5. MODIFYING SCHEME

It is ideal that the algorithm could stop automatically once some scale noise was removed, and the continued iteration of the Max/Min flow scheme would not produce further smoothing. Hence, a stricter stop criterion is required. Although does the scheme of Eq.(1) smooth out all the structures, the Max/Min flow scheme is a flexible computational framework. Its problem is that the decision rules in Eq.(1) are inapposite. It needs to be redefined. In fact, under the Max/Min flow scheme, we have two choices, one is to modify the curvature term and another is to redefine the decision rules.

Modified Scheme 1

First, we present a new scheme by redefining the decision rules. Consider the heat operator to be applied to the image intensity. Obviously, isotropic smoothing takes place in all directions. Sharp boundaries will be smeared. Conversely, the inverse heat equation could deblur or enhance an image. The famous example is the shock filter, in which the sign of the Laplacian, *sign*(*I*), is used to decide the evolving direction. Since the change of *sign*(Δ*I*) indicates that the current position should be on some boundaries. The reverse heat equation would enhance these boundaries. In the curvature motion equation, the diffusion should take place in the direction orthogonal to the gradient, whereas the boundaries in the gradient direction only need to be enhanced. This is easily fulfilled by replacing the Laplacian with the second derivative of image intensity in the direction of intensity gradient, $I_{\eta\eta}$, where is the direction of gradient. The scheme of Eq.(2) can be rewritten as,

$$F=\begin{cases}\max(\kappa,0), & \begin{cases}\text{average}\left(X\in\Omega(Y)\right)<Threshold\ \&\\ I(Y)<Threshold\ \&\\ edgef>0\end{cases}\\ 0, & otherwise\\ \min(\kappa,0), & \begin{cases}\text{average}\left(X\in\Omega(Y)\right)>Threshold\ \&\\ I(Y)>Threshold\ \&\\ edgef>0\end{cases}\end{cases} \quad (3)$$

where,

$$edgef=\max\left\{sign\left(\left(G_\sigma * I_{\eta\eta}\right)_X\right), X\in\Omega_{3\times3}(Y)\right\}\cdot\min\left\{sign\left(\left(G_\sigma * I_{\eta\eta}\right)_X\right), X\in\Omega_{3\times3}(Y)\right\},$$

where, G_σ is a Gaussian filter with variance σ^2. The *edgef* term in Eq.(3) is namely a zero-crossing detector based on the second derivative. When $edgef>0$, the edges are out of the detection window $\Omega_{3\times3}$. The diffusion takes place. On the other hand when $edgef\le 0$, the window $\Omega_{3\times3}$ should straddle the edges. So, no diffusion takes place. In practice, this kind of zero-crossing methods is usually implemented with the sophisticated canny edge detector. In this scheme, we firstly apply the canny detector on a sub-image centered around some point *Y* with *n* by *n* size. Then, the window $\Omega_{3\times3}(Y)$ around the point *Y* is defined on the output binary image from the canny detector. In this way, the *edgef* term becomes very simple.

It can be easily verified that when the current point is on some boundaries, the change of the sign of the second derivate stops the motion of the Max/Min flow. The further diffusion across the edges is suppressed. In this way, the sharp boundaries will be preserved, and smoothing would take place inside a region, but not across region boundaries. Hence, the scheme of (3) can reach a steady state solution.

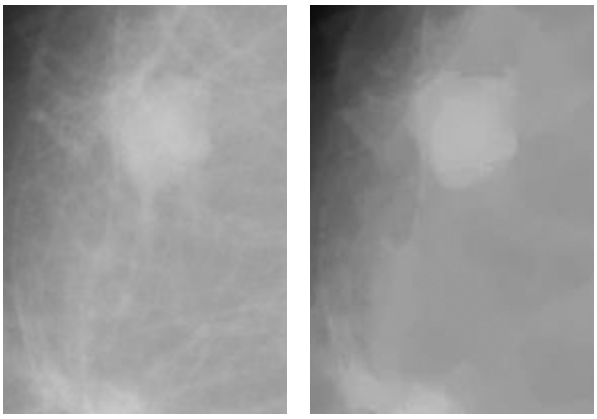

a. original image b. Using Eq.(3) with iteration=400

c. Using Eq.(2) with iteration=200

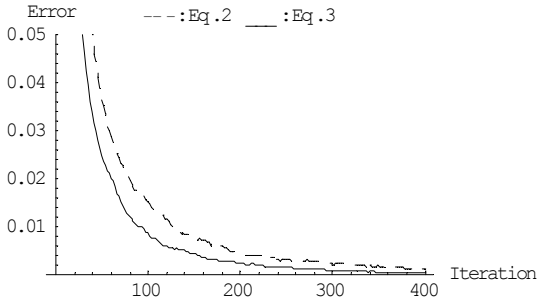

d. Error diagram

Fig. 6. Comparison of the evolution results using Eq.(2) and Eq.(3).

In Fig.6, we illustrate the evolution results of using the scheme of Eq.(2) and Eq.(3) with radius=1 on a mammographic image. Fig.6(d) demonstrates the scheme of Eq.(2) and Eq.(3) respectively reaching a steady state solution with the evolution error, which is calculated as, $error = \frac{1}{m \times n} \sum_{i,j}^{m,n} \left| I_{i,j}^{(t+1)} - I_{i,j}^{(t)} \right|$, where m and n are the width and height of image respectively. It can be noticed that the algorithm by Eq.(3) can stop automatically when all textures below the radius are removed, and the continued application of Eq.(3) will not produce further change. This should be contrasted with the results of applying Eq.(2), which can't terminate automatically, and will evolve into an image where the texture is smoothed and structure is eroded all along. In addition, it can be noticed that the effect of diffusion also relies on the zero-crossing detector. It is critical to select proper thresholds for the canny edge detector.

Modified Scheme 2

In the above presented scheme, the second derivate zero-cross detector is introduced to the decision rules under the Max/Min flow framework. As well, we yield the second presented scheme by introducing the gradient vector flow field to the curvature term.

The gradient vector flow (GVF) is computed as a diffusion of the intensity gradient vectors. In other words, the GVF is estimated directly from the continuous gradient space, and its measurement is contextual and not equivalent with the distance from the closest point. Thus, the noise can be suppressed. Besides that, the GVF provides a bi-directional force field that captures the object boundaries from either side. This provides a correct evolving direction for the curvature flow, and will lead to a steady state solution in the following presented scheme.

First, a Gaussian edge detector (zero mean, with σ_E variance) is used in the edge map defining [11],

$$f(\mathbf{x}) = 1 - \frac{1}{\sqrt{2\pi}\sigma_E} e^{\left(-\frac{|\nabla (G_\sigma * I)(\mathbf{x})|^2}{2\sigma_E^2} \right)}$$

The GVF field $\vec{\mathbf{v}}(\mathbf{x})$ is defined as the equilibrium solution to the following vector diffusion equation,

$$\begin{cases} \vec{\mathbf{v}}(\mathbf{x})_t = \mu \nabla^2 \vec{\mathbf{v}}(\mathbf{x}) - f(\mathbf{x})\left(\vec{\mathbf{v}}(\mathbf{x}) - \nabla f(\mathbf{x})\right)\left|\nabla f(\mathbf{x})\right|^2 \\ \vec{\mathbf{v}}(\mathbf{x},0) = \nabla f(\mathbf{x}) \end{cases}$$

where is a blending parameter. This field contains mainly contextual information and the flow vectors of this field always point to the closest object boundaries.

The $\vec{\mathbf{v}}(\mathbf{x})$ is dot-multiplied by the intensity norm vector, $\mathbf{N} = \frac{\nabla I}{|\nabla I|}$, as follows,

$$\vec{\mathbf{v}} \cdot \mathbf{N} = \lambda \nabla |\nabla I| \cdot \mathbf{N} = \lambda D^2 I \left\langle \frac{\nabla I}{|\nabla I|}, \mathbf{N} \right\rangle$$

where, $D^2 I$ denotes the Hessian of intensity I, and

$$\lambda(|\nabla I|) = \frac{|\nabla I|}{\sqrt{2\pi}\sigma_E^3} e^{\left(-\frac{|\nabla I|^2}{2\sigma_E^2} \right)} > 0$$

For the convenience, the Gaussian operator G_σ in $f(\mathbf{x})$ is omitted. Obviously, the above equation is equal to the second derivative of I in the direction of the intensity gradient, $I_{\eta\eta}$, up to a positive scale . The sign of $\vec{\mathbf{v}} \cdot \mathbf{N}$ will change along the normal to the boundaries in the neighborhood of boundaries even if the direction of gradient $\mathbf{N}$ doesn't change. Thus, the GVF indicates a correct evolution direction of the curvature flow, but not the intensity gradient. In Fig.7, the vector $\vec{\mathbf{v}}(\mathbf{x})$ in the GVF image always point to the closest boundaries of object.

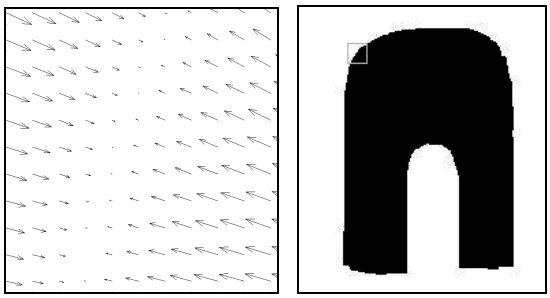

Fig.7 GVF field corresponding to the rectangle on right image

Obviously, the optimal way to reach the boundaries is to move along the direction of GVF. Given the fact that the propagation of the curvature flow always takes place in the inward normal direction, it is clear that the optimal propagation is obtained when the direction of $\vec{\mathbf{v}}(\mathbf{x})$ and the evolving direction of the original curvature flow from

the observed images, $-\mathbf{N}$, are identical. Because of the noise or spurious edge, the evolving direction of the curvature flow can't always align to the $\vec{\mathbf{v}}(\mathbf{x})$. Hence, the worse case occurs when the $\vec{\mathbf{v}}(\mathbf{x})$ is tangent to the evolving direction. However, the correct curvature flow can be defined by their inner product as follows,

$$\hat{\kappa} = sign\left(-\vec{\mathbf{v}} \cdot \kappa\mathbf{N}\right)\kappa$$

Under the Max/Min flow framework, we have

$$F = \begin{cases} \max(\hat{\kappa},0), & \begin{cases} \text{average}\left(X \in \Omega(Y)\right) < Threshold \\ I(Y) < Threshold \end{cases} \\ 0, & otherwise \\ \min(\hat{\kappa},0), & \begin{cases} \text{average}\left(X \in \Omega(Y)\right) > Threshold \\ I(Y) > Threshold \end{cases} \end{cases} \quad (4)$$

From the proposition 2, we know the curvature flow under the Max/Min flow framework will smooth out all structure except the edges of shape over the boundary of the whole images. When the curvature flow is replaced by $\hat{\kappa}$, it is obvious that the evolving direction of the curvature flow should be determined by $sign\left(-\vec{\mathbf{v}} \cdot \kappa\mathbf{N}\right)$. Consider a small neighborhood of some point on the boundaries of shape Ω. For some point $X \in \Omega$, we assume that the intensity curvature >0 and the GVF and the evolving direction of the curvature flow have the same direction, i.e. $sign\left(-\vec{\mathbf{v}} \cdot \kappa\mathbf{N}\right) = 1$. If the max flow is selected according to the decision rules in Eq.(4), the convex in Ω is smoothed. The curvature flow runs across the boundary of shape. Then, in the next iteration, the GVF and the evolving direction of the curvature flow have opposite directions, i.e. $sign\left(-\vec{\mathbf{v}} \cdot \kappa\mathbf{N}\right) = -1$. Even if the max flow is selected according to the decision rules in Eq.(4), the speed function is set to zero, i.e. $F = 0$, and therefore any the further diffusion would be suppressed. So, the final steady state image should contain the essential structures of the shape.

In fact, the flow under $F = \hat{\kappa}$ is namely the shock filter. Expanding $\hat{\kappa}$, we yield,

$$\begin{aligned} \hat{\kappa} &= -sign\left(\lambda D^2 I\left\langle \frac{\nabla I}{|\nabla I|}, \mathbf{N} \right\rangle\right)|\kappa| \\ &= -sign(\lambda I_{\eta\eta})|\kappa| \end{aligned}$$

and its evolution equation, $I_t = -sign(\lambda I_{\eta\eta})|\kappa|\|\nabla I|$. Clearly this is the standard shock filter equation up to a positive scale $|\kappa|$. The scheme of (4) may be viewed as an implementation of the shock filter under the max/min flow framework. As a matter of fact, the classical shock filter is extremely sensitive to noise. Whereas, the scheme of Eq.(4) performs well on enhancing and denoising.

The distinct advantage of the GVF fields is to provide a large capture range for the edges. This is in favor of denoising. Thus, we illustrate the scheme of (4) on the noisy and blurred image. In Fig.8, we show the evolution results of applying our presented scheme of (4) on the same mammographic image as in Fig.6. The original image is degraded with Gaussian noise (zero mean, with 0.1 variance) in Fig.8(b). Fig.8(d) demonstrates the scheme of Eq.(4) reaching a steady state solution with the evolution error diagram. Obviously, the presented scheme can effectively remove noise while preserving some essential features of object simultaneously. The original medical image is very blurry, and its luminous contrast is very low. In order to illustrate the properties of the scheme (4), we apply this scheme on a nature scene image, so that its advantages become evident. In Fig.9(b), the original water lily image is blurred and degraded with Gaussian noise. We can see that the features of the lily image are enhanced effectively, and the final steady state image can preserve the essential details. In addition, the final effect of diffusion also relies on the GVF fields. The ideal case is that all the essential details of shape should be preserved in the GVF fields.

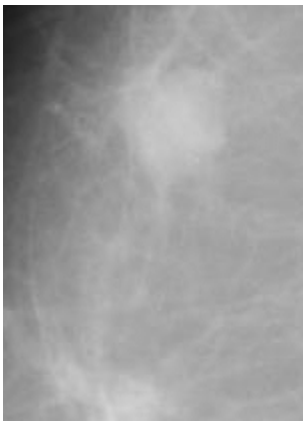

a. Original image

b. Gaussian noisy image

c. iteration=400

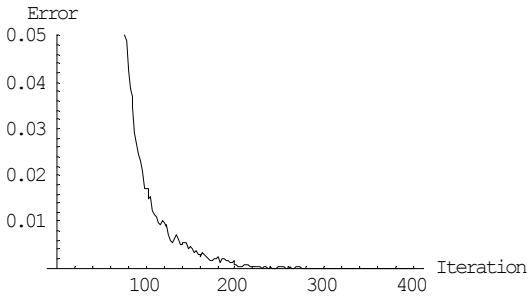

d. Error diagram

Fig.8 Applying Eq.(4) on the Gaussian noisy image

a. original image b. blurring and adding Gaussian noise

c. iteration=200

Fig.9 Water lily image is restored

6. CONCLUSIONS

In this paper, we studied the image enhancement and denoising under the Max/Min flow framework, and solved the speckle problem under the proposed reformulated Max/Min flow framework. Furthermore, we proved that the continued application of the original scheme would erode all structures or boundaries for the grey-level (or color) image. In order to control smoothing effect, the zero-crossing detector and GVF field are introduced in the curvature flow, so that the proposed schemes can reach a steady state solution respectively, and the final steady state image maintains the essential structures of the shape while the small oscillations are smoothed out.

From the experiment results of the medical image, the edge contrast is not enough. Thus, we will try to introduce the inverse diffusion equation to the proposed scheme in future work.

REFERENCES

[1] P.Perona and J.Malik, Scale-space and edge detection using anisotropic diffusion, IEEE Trans. On PAMI, Vol. PAMI-12, No.7, pp.629-639, 1990

[2] S.Osher and L.Rudin, Feature-oriented image enhancement using shock filter, SIAM J. of Numer. Anal. Vol.27, pp.919-940, 1990

[3] L.Rudin, S.Osher and E.Fatemi, Nonlinear total variation based noise removal algorithms, Physica D, Issues 1-4, Vol.60, pp.259-268, 1992

[4] L.Alvarez, P.-L.Lions and J.-M.Morel, Image selective smoothing and edge detection by nonlinear diffusion (II), SIAM, J. of Numer. Anal., Vol.29, No.3, pp.845-866, 1992

[5] Y.G.Chen, Y.Giga and S.Goto, Uniqueness and existence of viscosity solutions of generalized mean curvature flow equations, J. of Difference Geometry, Vol.33, No.3, 1991

[6] R.Malladi and J.A.Sethian, Image Processing: flows under Min/Max curvature and mean curvature, Graphical models and image processing, Vol.58, No.2, pp.127-141, 1996

[7] R. Malladi and J.A. Sethian, A unified approach to noise removal, image enhancement, and shape recovery, IEEE Trans. On Image Processing, Vol.5, No.11, pp.1554-1568, 1996

[8] B.B.Kimia, A.Tannenbaum and S.W.Zucker, On the evolution of curves via a function of curvature I: the classical case, J. of Mathematical analysis and applications, Vol.163, No.2, pp.438-458, 1992

[9] G.Shapiro and A.Tannenbaum, Affine invariant scale-space, Int'l. J. of Computer Vision, Vol.11, No.1, pp.25-44, 1993

[10] C.Xu and J.Prince, Snakes, shapes, and gradient vector flow, IEEE Trans. On Image Processing, Vol.7, No.3, pp.359-369, 1998

[11] N.Paragios, O.Mellina-Gottardo and V.Ramesh, Gradient vector flow fast geodesic active contours, in Proceedings of IEEE Int'l Conf. On Computer Vision, Vol.1, pp.67-73, Vancouver, Canada, 2001

ACKNOWLEDGEMENT

This research work was also supported by the Natural Science Foundation of China under grant 60203003.